Realistische Simulation spezifischer CT-Systeme in aRTist 2
Realistic Simulation of Specific CT-Systems in aRTist 2

Florian WOHLGEMUTH [1], Tino HAUSOTTE [1]
[1] Lehrstuhl für Fertigungsmesstechnik (FMT), Friedrich-Alexander-Universität Erlangen-Nürnberg (FAU), Erlangen

Kontakt E-Mail: Florian.Wohlgemuth@fmt.fau.de

Kurzfassung. Die Simulation röntgencomputertomografischer Messungen verspricht vielfältige Anwendungsmöglichkeiten wie die numerische Messunsicherheitsbestimmung, simulative Aufnahmeplanung/-optimierung und die Vorhersage (sowie darauf basierende Korrektur) von systematischen Messabweichungen bzw. Artefakten. Alle diese Anwendungspotentiale benötigen eine möglichst realitätsgetreue Simulation. Die Software aRTist 2 der Bundesanstalt für Materialforschung und –prüfung (BAM) ist eine Simulationsplattform für virtuelle Radiografie und CT-Aufnahmen. Um ein spezifisches reales CT-System nachzubilden, ist eine entsprechende Parametrisierung in aRTist 2 notwendig. Hierfür gibt es bisher keine vollständige systematische Vorgehensweise – die Simulation eines konkreten realen CT-Systems ist oft Resultat eines aufwendigen individuellen Anpassungsprozesses, der zeitaufwändig und fehleranfällig ist.

Im Beitrag werden systematische Vorgehensweisen beschrieben, mit denen auf Basis einer definierten Anzahl von Projektionsmessungen am realen CT-System eine realistische Simulation der Effekte von Brennfleck, Detektorunschärfe und Detektorcharakteristik möglich ist. Verschiedene Bestimmungsverfahren für die Effekte werden diskutiert. Dabei wird der Schwerpunkt nicht auf die möglichst realistische Charakterisierung des CT-Systems, sondern auf die Bestimmung von Parametern, die dessen Verhalten möglichst genau simulierbar machen, gelegt. Daher wird die Detektorcharakteristik als klassisches Datenregressionsproblem verstanden, bei dem gemessene Projektionsgrauwerte durch eine Minimierung möglichst gut in der Simulation wiedergegeben werden. Weiterhin wird anhand von Messungen hinterfragt, inwiefern das Grauwertrauschen realer Projektionen sinnvoll wiedergeben werden kann.

Als Ausblick wird diskutiert, welche weiteren Schritte für die Parameterbestimmung und Parametrisierung der Simulation notwendig sind. Als Fernziel soll auf Basis definierter Messprozeduren eine wiederholbare und übertragbare Vorgehensweise geschaffen werden, mit der die Simulation eines realen CT-Systems ohne individuellen, iterativen Anpassungsprozess möglich ist. Dies würde den Nutzen und die Anwendbarkeit der CT-Simulation deutlich erhöhen bzw. erleichtern.

Introduction

The simulation of industrial X-ray computed tomography (CT) measurements would potentially allow numerous applications like numerical measurement uncertainty evaluation, simulative measurement parameter optimisation and correction of artefacts using simulative predictions. All of these applications require a faithful simulation. There are simulation platforms available – e.g. Scorpius XLab by Fraunhofer EZRT (Fürth, Germany) [1], CIVA CT [2], SimCT by FH OÖ (Wels, Austria) [3] or aRTist by BAM (Berlin, Germany) [4]. The latter is used for the purpose of this article. All of these simulation platforms simulate the physical radiographic processes and allow for the parametrisation of different acquisition scenarios. They do however not provide a faithful simulation of any given real CT system out of the box as the parametrisation is still challenging.

After a general overview of the problem, this article describes systematic approaches to capture some elements of the real CT system behaviour faithfully and parametrise them in aRTist.

1. Challenges for the Simulation of Specific CT Systems

An overview of the necessary steps for CT system parameterisation – i.e., the determination of parameters for a simulation platform that will enable faithful and realistic simulations of a specific real CT system – has been given in [5]. The measurement object needs to be represented as a geometric model as input for the simulation. This in itself can be challenging for non-destructive testing purposes if e.g. pores have to be simulated realistically [6]. For dimensional metrology purposes, a CAD model is often available and can be used. It is useful for the exact material composition to be known as even small fractions can influence the attenuation characteristics [5].

For the CT system itself, the parametrisation can be roughly subdivided into the X-ray source properties, the detector properties and the geometrical behaviour of the system. Obviously, further system properties might be relevant for selected use cases or selected CT systems, therefore this categorisation should not be understood as exhaustive.

For the X-ray source, the most obvious characteristic is its spectrum. There are multiple spectrum estimation tools available (see e.g. [7,8]). For the purpose of this discussion, they will be considered adequate. A characteristic of real X-ray sources that these spectrum estimators do usually not capture is angular anisotropy of the flux or spectrum – if this effect proves relevant and cannot be modelled in another fashion, this is a possible source of deviations between a simulation and real CT systems. The X-ray source is usually a X-ray tube with a target on which incident electrons cause X-ray radiation. To limit the thermal stress on the target, the incident electron ray is usually defocused, leading to a focal spot, which blurs the projection. The focal spot size and shape are therefore important CT system properties that need to be captured by the simulation. Simple edge-projection-based methods can already yield some information about the focal spot size but are limited concerning their information about the focal spot shape [9,10]. A method recently rediscovered for industrial computed tomography systems is the single shot focal spot reconstruction [11-13]. A circular aperture is X-rayed at a high magnification and edge grey value profiles in all directions are collected around the projected circle (compare Figure 1). The derivatives of those edge profiles are a rescaled version of the Radon transform of the focal spot shape and therefore allow for reconstruction of the focal spot.

All properties of the source can change over time (e.g. due to thermal load). This change needs to be characterised and accounted for in the simulation if it happens during the time scale of one scan.
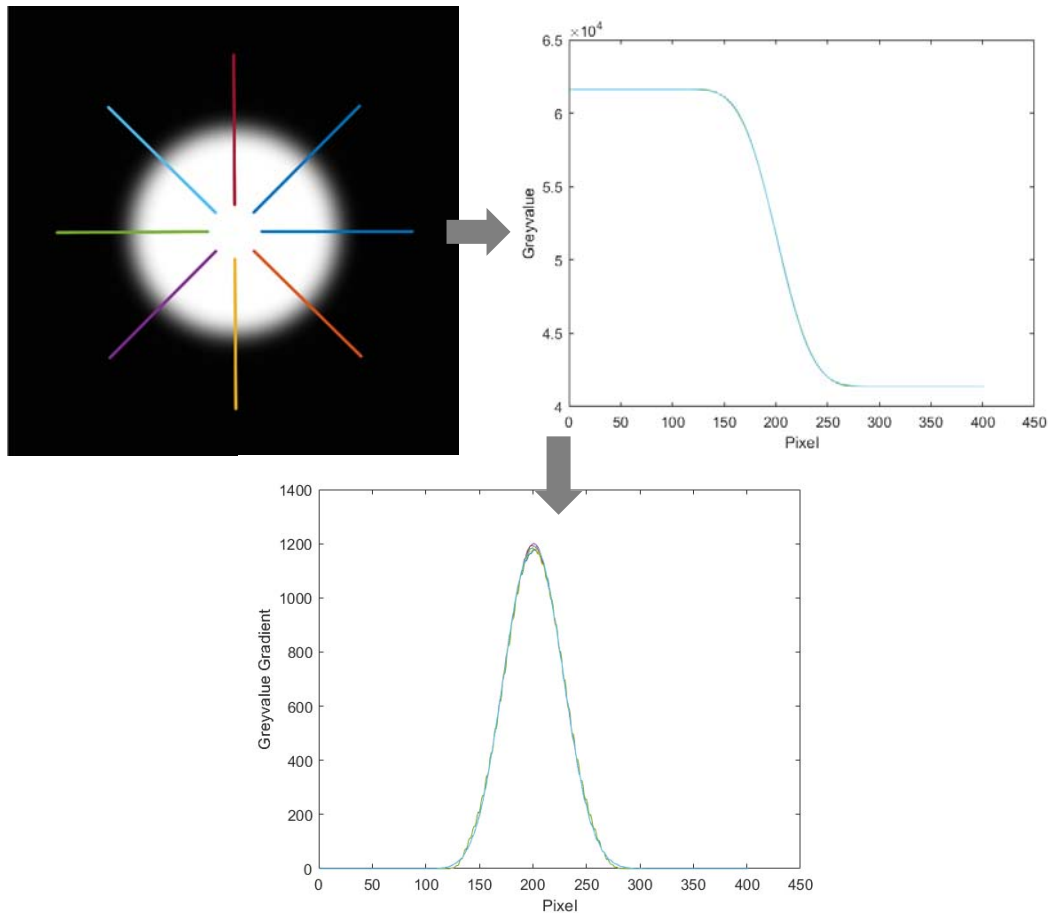
Fig. 1. Illustration of the focal spot CT method. The projection of a circular aperture is acquired and the edge profiles along the circle are extracted. The derivatives of these edge profiles are calculated and can be used as input data for a planar reconstruction of the focal spot shape.

For the detector, spectral response (compare section 2.1) and noise behaviour (compare section 2.2) are important properties that need to be modelled. Furthermore, the detector has a certain inherent unsharpness that can be measured using edge profiles [9,10] or adequate standardised methods [14-16]. Detectors can further exhibit effects like afterglow, internal scatter or fluorescence, which will not be discussed here. If these effects are relevant, they need to be included in the simulation model as well.

The geometrical behaviour of the CT system entails both the system acquisition geometry and the deviations from the acquisition setup occurring during a typical CT scan. While the system acquisition geometry is usually well known due to system qualification procedures and because it is needed for the reconstruction of the acquired projections, the deviations from this assumed acquisition geometry are rarely characterised, much less available to the end-user wanting to simulate their CT system. There are approaches to determine these by evaluating projections (see e.g. [17-19]), but this topic will not be discussed in detail in this article.

For all properties listed in this section – both of the scanned object as well as the CT system – it is currently unclear how accurate they need to be modelled in a simulation software for which purpose. It is plausible that for different applications, different levels of accuracy will suffice. As long as there is little experience on that matter, it does seem instructive to aim for an accurate modelling of each property the real CT system does exhibit. Reducing the effort in modelling single parameters or properties is easily feasible once the whole simulation model yields realistic results analysing the perturbation of single parameters and deriving (task-specific) parameter sensitivities. This can however only be done once the whole simulation model is resulting in realistic projections – single parameter

studies have limited significance for the necessary accuracy as they cannot capture correlation effects.

2. Realistic Modelling of Detector Properties

Section 2.1 summarises an approach to derive a detector characteristic for the simulation from measured projection data. Section 2.2 describes characterisation measurements of the noise behaviour of a real CT system.

2.1 Spectral Detector Characteristic

In principle, the single parts of the detector can be modelled as faithfully as possible e.g. in a physical particle transport Monte Carlo simulation or using models as proposed in [20]. A different approach is to treat the detector as a black box and try to find model parameters within the simulation approach that reproduce measured data as well as possible. We have done this in [21]. The approach is based on measuring attenuation sequences of a material with increasing material thickness at different tube voltage-/current-settings and extracting different lines of calculated energy density-grey value characteristics for each voltage-/current-setting. A spectral characteristic – that modifies the energy density values – is then obtained by an optimisation procedure with the difference between the different characteristics as a minimisation target function. The resulting spectral characteristic allows the simulation to reproduce the grey values of the projections for all different voltage-/current-settings. Details on the approach can be found in [21].
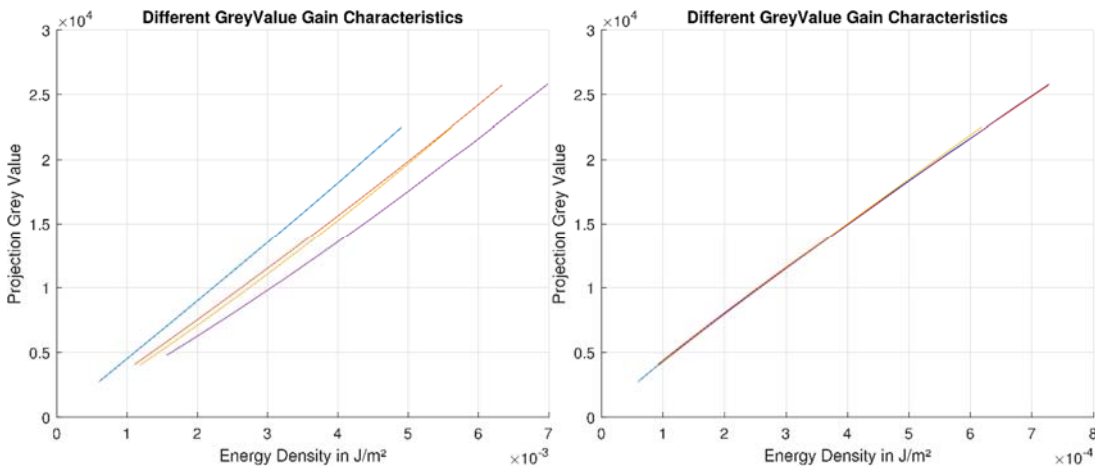

Fig. 2. Left: Measured average projection grey values versus energy densities calculated without any spectral sensitivity. Right: Measured average projection grey values versus energy densities calculated with optimised spectral sensitivities. The optimisation procedure is therefore able to reproduce the spectral response of the real detector in the simulation. Taken from [21].

2.2 Image Noise in Projections

In projections of CT scans, there are multiple sources for grey value noise. Stolfi *et al.* name four categories: random noise, quantum noise, electronics noise and round-off noise [22]. This noise is a contribution to the measurement uncertainty [23] and thus, an important characteristic that the simulation should be able to reproduce. Consequently, we wanted to inspect the noise characteristic of real projections to know how they should look. We therefore measured projections with empty measurement volume at different settings using the Zeiss (Oberkochen, Germany) Metrotom 1500 at the Institute of Manufacturing

Metrology. For each setting, we measured around 1 000 projections to be able to see the noise behaviour of each single pixel. Figure 3 shows the pixel-wise standard deviation of the grey values at tube settings of 180 kV and 180 μA based on 1 000 projections. The projections are flatfield-/gain-corrected. It is visually clear that the noise is non-ergodic – i.e., the ensemble noise and the single pixel noise are not the same. The projection noise can therefore not be characterised by inspecting single projections as this would neglect the spatial dependence of the noise.
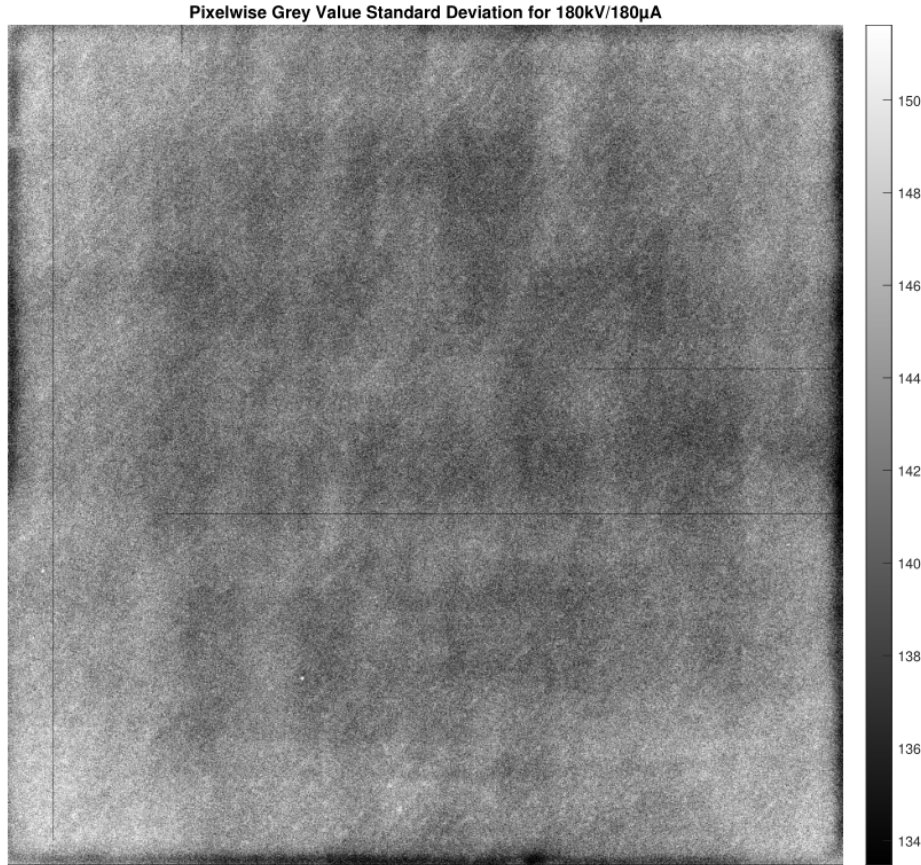

Fig. 3. Pixel-wise standard deviation of the grey values at tube settings of 180 kV and 180 μA based on 1 000 projections. A 0.25 mm Cu filter was used. The detector settings are 1 000 ms acquisition time, 16 x gain and no binning or image averaging.

The single pixel grey values show distributions that are compatible with a normal distribution hypothesis according to Kolmogorov-Smirnov, Lilliefors, Anderson-Darling and Jarque-Bera test for almost all pixels (rejection percentages below 0.02 % for all settings and all tests). The patterns (as seen in Figure 3) seems to be characteristic for the detector as, visually, they all seem to have a high degree of similarity (for various different tube settings). To quantify this, ratio maps were created. These ratio maps $P_R(i,j)$ (with i,j denoting the pixel indices) are calculated according to:

$$P_R(i,j) = \frac{P(i,j)}{R(i,j)}$$

Here, $R(i,j)$ is the standard deviation image of a 'reference' setting and $P(i,j)$ the standard deviation image of the setting under inspection.

For the tube setting of 140 kV and 360 μA, the ratio map is shown in Figure 4. It is remarkable that all patterns seen in the noise image in figure 3 (which are similarly present in the noise image for 140 kV and 360 μA (not shown)) vanish and the ratio map exhibits visually pattern-free variations. This is interpreted as another indicator that the noise patterns

are indeed characteristic for the detector and can be modelled accordingly. Similar ratio maps result for most other measurement settings tested.
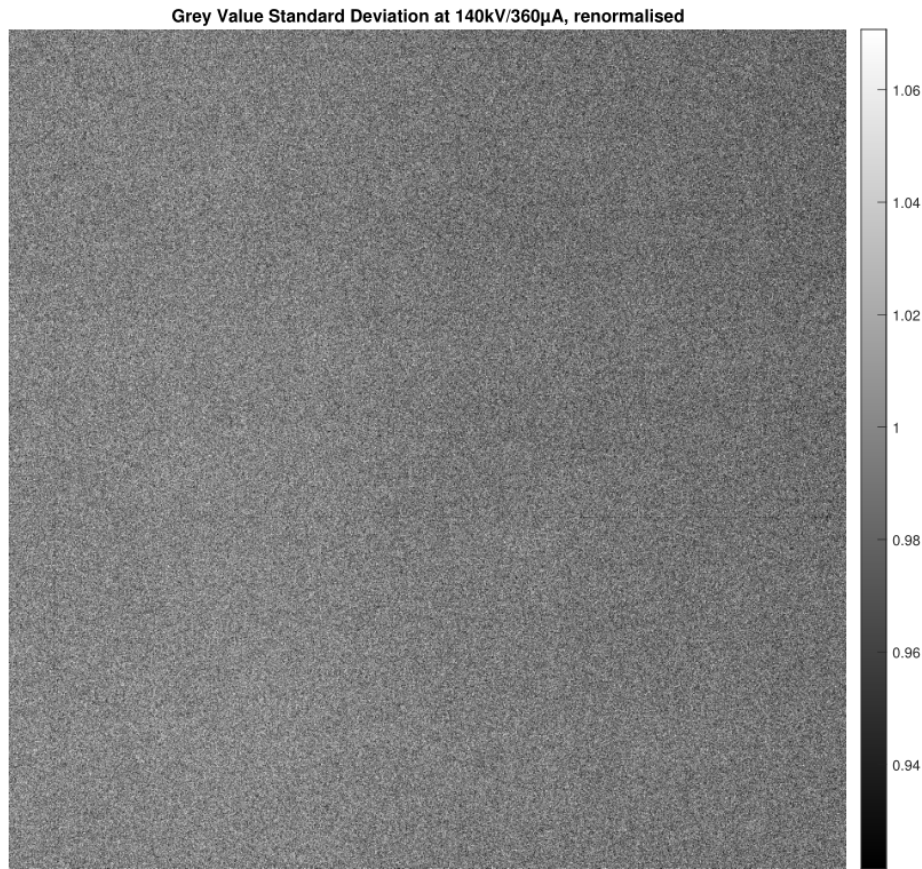

Fig. 4. Ratio of pixel-wise grey value standard deviation of the measurement at tube settings of 140 kV and 360 μA and the measurement at tube settings of 180 kV and 180 μA (as reference; settings as in figure 3). It is worth noting that there are no clear patterns in the resulting image.
The acquisition settings are 0.25 mm Cu filter, 1 000 ms acquisition time, 16 x gain and no binning or image averaging.

Motivated by these apparent similarities, we rescaled each standard deviation image for the different settings by dividing by its own mean value. As a result, we obtained different rescaled noise pattern images that have a high similarity. This means that, phenomeno-logically, the noise could be simulated by using one single Gaussian distribution (with the mean standard deviation appropriate for the tube and detector settings) for the whole detector and then multiplying the resulting noise image by the rescaled map which captures the actual spatial noise distribution the real projections exhibit. This would permit transferring the real spatial distribution of the noise onto the simulated projections.

3. Conclusions

Section 1 summarised the challenges and steps necessary to parameterise a real CT system in a radiographic simulation platform. In section 2, an approach for spectral sensitivity determination of the detector using measured projections as well as an approach to transfer real projection noise characteristics onto simulated projections were presented. It was shown that projection noise is non-ergodic, meaning that an accurate characterisation is not feasible using a single projection but will be a time-intensive process. The actual implementation of

the transfer of the noise characteristics onto simulated projections will be a future step of research.

Acknowledgements

Author Contributions according to CASRAI CRedit Taxonomy [24]

F. W. contributed Conceptualization, Data curation, Formal Analysis, Investigation, Methodology, Software, Visualization as well as Writing - original draft. Both T. H. and F. W. contributed to Funding acquisition and Project administration. T. H. contributed Resources, Supervision and Writing - review & editing.

References

[1] J. Hiller, T. Fuchs, S. Kasperl and L. Reindl, "Einfluss der Bildqualität röntgentomographischer Abbildungen auf Koordinatenmessungen Grundlagen, Messungen und Simulationen", Technisches Messen, Vol. 78, pp. 334-347 (2011)
[2] Extende, "COMPUTED TOMOGRAPHY WITH CIVA", <http://www.extende.com/computed-tomography-with-civa/> (05.05.2020)
[3] M. Reiter, M. Erler, C. Kuhn, C. Gusenbauer and J. Kastner, "SimCT: A simulations tool for X-ray imaging", NDT.net issue, Vol. 21, No. 02, (2016)
[4] C. Bellon, K. Burger and C. Gollwitzer, "Virtual CT acquisition and reconstruction of complex and noisy scanning trajectories in aRTist", Proceedings of the 9th Conference on Industrial Computed Tomography, Padova, Italy (2019)
[5] F. Wohlgemuth, F. Wolter, and T. Hausotte, "Digitale Zwillinge metrologischer Röntgencomputertomografen für die numerische Messunsicherheitsbestimmung," in ZfP heute. Wissenschaftliche Beiträge zur zerstörungsfreien Prüfung 2020, Ed. 2020, pp. 106–110
[6] P. Fuchs, T. Kröger, T. Dierig, and C. S. Garbe, "Generating Meaningful Synthetic Ground Truth for Pore Detection in Cast Aluminum Parts," in 9th Conference on Industrial Computed Tomography, Padova, Italy, 2019
[7] C. Leinweber, J. Maier, and M. Kachelrieß, "X-ray spectrum estimation for accurate attenuation simulation", Medical Physics, 44 (12), pp. 6183–6194, 2017
[8] Deresch, "Modellierung von Röntgenspektren für technische Anwendungen", Universität Potsdam, 2015
[9] M. Fleßner, M. Blauhöfer, E. Helmecke, A. Staude, and T. Hausotte, "CT measurements of microparts: Numerical uncertainty determination and structural resolution", in: SENSOR 2015, Nürnberg, 2015

[10] C. Orgeldinger, F. Wohlgemuth, A. Müller, and T. Hausotte, "Spot size and detector unsharpness determination for numerical measurement uncertainty determination", in: 9th Conference on Industrial Computed Tomography, Padova, Italy, 2019.

[11] G. D. Domenico, P. Cardarelli, A. Contillo, A. Taibi, and M. Gambaccini, "X-ray focal spot reconstruction by circular penumbra analysis-Application to digital radiography systems", Medical Physics, 43 (1), pp. 294–302, 2015

[12] U. Ewert, G.-R. Jaenisch, A. Deresch, B. A. Bircher, and F. Meli, „Neue Konzepte zur Messung von Parametern der Brennflecke von Nano- und Mikrofokus-Röntgenröhren", in: DACH-Jahrestagung 2019, 2019

[13] U. Ewert, G.-R. Jaenisch, A. Deresch, B. A. Bircher, and F. Meli, "New Concepts for the Measurement of Focal Spot Parameters of Nano- and Microfocus X-Ray Tubes", in: International Symposium on Digital Industrial Radiology and Computed Tomography – DIR2019, 2019

[14] ASTM E2597/E2597M – 14

[15] ASTM E2002 – 15

[16] DIN EN ISO 19232-5:2018-12, Zerstörungsfreie Prüfung – Bildgüte von Durchstrahlungsaufnahmen – Teil 5: Bestimmung der Bildunschärfezahl mit Doppeldraht-Typ-Bildgüteprüfkörpern (ISO 19232-5:2018)

[17] B. A. Bircher , F. Meli , A. Küng , R. Thalmann, "CT geometry determination using individual radiographs of calibrated multi-sphere standards", in: 9th Conference on Industrial Computed Tomography, Padova, Italy (iCT 2019)

[18] B. A. Bircher, F. Meli, A. Küng, R. Thalmann, "X-ray source tracking to compensate focal spot drifts for dimensional CT measurements", in: 10th Conference on Industrial Computed Tomography, Wels, Austria (iCT 2020)

[19] M. Ferrucci, "Systematic approach to geometrical calibration of X-ray computed tomography instruments", KU Leuven, 2018

[20] J. Hiller, "Abschätzung von Unsicherheiten beim dimensionellen Messen mit industrieller Röntgen-Computertomographie durch Simulation". IMTEK, University of Freiburg, 2011.

[21] F. Wohlgemuth, C. Bellon and T. Hausotte, "Measurement-based Detector Characteristics for Digital Twins in aRTist". WCNDT2020, South Korea 2022 (accepted)

[22] A. Stolfi, L. De Chiffre and S. Kasperl, "Error Sources", in: S. Carmignato, W. Dewulf, R. Leach, "Industrial X-Ray Computed Tomography", Springer, Cham, 2018

[23] A. Rodríguez-Sánchez, A. Thompson, L. Körner, N. Brierley, R. Leach, "Review of the influence of noise in X-ray computed tomography measurement uncertainty", Precision Engineering 66 (2020) 382–391

[24] CASRAI, CRediT, available on https://casrai.org/credit/ (accessed 16.03.2021)